ANTIMICROBIAL AGENTS AND CHEMOTHERAPY, June 2005, p. 2445–2453 Vol. 49, No. 6
0066-4804/05/$08.00+0 doi:10.1128/AAC.49.6.2445–2453.2005

Antifungal Protein PAF Severely Affects the Integrity of the Plasma Membrane of *Aspergillus nidulans* and Induces an Apoptosis-Like Phenotype

Éva Leiter,[1] Henrietta Szappanos,[2] Christoph Oberparleiter,[3] Lydia Kaiserer,[3] László Csernoch,[2] Tünde Pusztahelyi,[1] Tamás Emri,[1] István Pócsi,[1] Willibald Salvenmoser,[4] and Florentine Marx[3]*

Department of Microbiology and Biotechnology, Faculty of Science,[1] and Department of Physiology, Research Center for Molecular Medicine, Medical and Health Science Center,[2] University of Debrecen, Debrecen, Hungary; Biocenter, Division of Molecular Biology, Innsbruck Medical University, Innsbruck, Austria[3]; and Institute of Zoology and Limnology, Division of Ultrastructure and Evolutionary Biology, University of Innsbruck, Innsbruck, Austria[4]

Received 20 August 2004/Returned for modification 24 August 2004/Accepted 9 February 2005

The small, basic, and cysteine-rich antifungal protein PAF is abundantly secreted into the supernatant by the β-lactam producer *Penicillium chrysogenum*. PAF inhibits the growth of various important plant and zoopathogenic filamentous fungi. Previous studies revealed the active internalization of the antifungal protein and the induction of multifactorial detrimental effects, which finally resulted in morphological changes and growth inhibition in target fungi. In the present study, we offer detailed insights into the mechanism of action of PAF and give evidence for the induction of a programmed cell death-like phenotype. We proved the hyperpolarization of the plasma membrane in PAF-treated *Aspergillus nidulans* hyphae by using the aminonaphtylethenylpyridinium dye di-8-ANEPPS. The exposure of phosphatidylserine on the surface of *A. nidulans* protoplasts by Annexin V staining and the detection of DNA strand breaks by TUNEL (terminal deoxynucleotidyltransferase-mediated dUTP-biotin nick end labeling) gave evidence for a PAF-induced apoptotic-like mechanism in *A. nidulans*. The localization of reactive oxygen species (ROS) by dichlorodihydrofluorescein diacetate and the abnormal cellular ultrastructure analyzed by transmission electron microscopy suggested that ROS-elicited membrane damage and the disintegration of mitochondria played a major role in the cytotoxicity of PAF. Finally, the reduced PAF sensitivity of *A. nidulans* strain FGSC1053, which carries a dominant-interfering mutation in *fadA*, supported our assumption that G-protein signaling was involved in PAF-mediated toxicity.

A large number of small, basic, cysteine-rich antimicrobial proteins are produced by organisms throughout all kingdoms. They display a great variety in their primary structure, in species specificity, and in the mechanism of action.

Few ascomycetes secrete strongly related antifungal proteins, which do not show any sequence homology with other antimicrobial proteins, but most of these proteins exhibit structural similarities (46): a net positive charge and numerous cysteine residues that are involved in disulfide bond formation. These properties contribute to a compact tertiary structure and a high stability against environmental impact and finally support the model of a membrane-disturbing nature. The antifungal protein PAF from *P. chrysogenum* and AFP from *A. giganteus* are the two most intensively studied peptides in the group of antifungals from ascomycetes, but the information available on their exact mechanism of action is still rather limited (32, 55, 68, 69). PAF inhibits the growth of various important plant pathogenic and zoopathogenic filamentous fungi, e.g., *Aspergillus fumigatus*, *A. niger*, *A. nidulans*, and *Botrytis cinerea*. Previous studies revealed the induction of multifactorial detrimental effects on target organisms that include growth inhibition, reduction of cellular metabolism, severe changes in hyphal morphology, increased K^+ efflux, and the generation of intracellular reactive oxygen species (ROS) (32, 48). PAF was found to be actively internalized by target molds and to localize to the cytoplasm, possibly evoking deleterious effects from inside the cell (55). This led us to the assumption that PAF may have intracellular targets and that permeabilization of microbial membranes may be a secondary effect rather than the primary cause of antifungal activity.

The accumulation of intracellular ROS can have severe impact on cells, i.e., the random oxidation of the whole range of biopolymers including proteins, lipids, nucleic acids, and the destruction of cellular membranes and organelles, such as mitochondria (12, 35). When the accumulation of oxidative cell damages threatens basic physiological functions, programmed cell death (PCD) processes are likely to be put up to operation (45, 53, 65). Apoptosis or apoptosis-like cell death is carefully regulated and occurs as either an inherent part of development or can be triggered by various external signals, i.e., toxins, receptor ligand binding and different kinds of environmental stress. The onset of PCD finally leads to a characteristic phenotype showing phosphatidylserine (PS) externalization, membrane blebbing, increased vacuolization, DNA and nuclear fragmentation, and apoptotic body formation. Although apo-

* Corresponding author. Mailing address: Biocenter, Division of Molecular Biology, Innsbruck Medical University, Fritz-Pregl Strasse 3, A-6020 Innsbruck, Austria. Phone: 43-512-5073607. Fax: 43-512-5079880. E-mail: florentine.marx@uibk.ac.at.

ptosis was confined to multicellular higher eukaryotes in the past, there is increasing body of evidence that lower eukaryotes such as filamentous fungi, e.g., *A. fumigatus*, *A. nidulans*, and unicellular organisms such as yeasts, also show characteristics of apoptosis-like cell death under certain circumstances (16, 43, 51, 52).

A. fumigatus is the most severe zoopathogen among all *Aspergilli* (37), and its genes exhibit strong structural and functional similarities with those of the model organism *A. nidulans* (6, 21). Nevertheless, *A. fumigatus* is still less well studied than *A. nidulans* and well-defined mutants are rare. Therefore, we used *A. nidulans* in the present study and show that PAF-mediated toxicity evokes a complexity of physiological changes including the hyperpolarization of cellular membranes, the intracellular accumulation of ROS, disintegration of mitochondria (mitoptosis) and finally an apoptosis-like cell death. Furthermore, the PAF resistance of the *A. nidulans* strain *fadA*^{G203R}, which carries a dominant-interfering mutation in the α-subunit of the heterotrimeric G protein, implies that PAF toxicity may depend on the disturbance of FadA G-protein signaling. The elucidation of the underlying mechanism by which PAF induces cell death in target fungi could be beneficial for future antifungal drug design.

MATERIALS AND METHODS

Strains and culture conditions. The following strains used in the present study were purchased from the Fungal Genetic Stock Center (University of Kansas Medical Center): wild-type (wt) FGSC A4 (*veA*$^{+}$) and FGSC26 (*biA veA1*); RJH046 (*argB2 biA1 pyroA4 veA1* Δ*flba*::*argB*) and FGSC1035 (*yA2 fadA*^{G203R}), which both carry mutations in components of FadA/FlbA G-protein signaling; and FGSC33 (*biA1 pyroA4 veA1*) and FGSC116 (*yA2*), which are the corresponding control parent strains for RJH046 and FGSC1035, respectively. All strains were cultivated in YPD medium (2% peptone, 1% yeast extract, 2% glucose) at 30°C. For the preparation of protoplasts, 100 ml of minimal nitrate medium (pH 6.5) (4) supplemented with 0.5% yeast extract was inoculated with 5×10^7 conidia. Cultures were incubated at 37°C for 16 h on an orbital shaker (200 rpm). For fluorescence staining, *A. nidulans* was grown overnight on glass coverslips at 30°C in YPD inoculated with 10^6 conidia/ml.

Determination of antifungal activity. The antifungal protein PAF was purified from the supernatant of a 72-h culture of *P. chrysogenum* Q176 as described elsewhere (47). The activity assays were performed according to the protocols of Broekaert et al. (10) and Ludwig and Boller (42). In brief, conidia were diluted in YPD to 10^3 to 10^4/ml in 96-well plates. Serially diluted PAF solutions were added to each well, and cell suspensions were incubated in a total volume of 200 μl for various time points at 25°C (room temperature). To test the PAF activity in the presence of guanidine nucleotide analogs, 100 μM GTPγS, GDPβS, and ATPγS (Sigma-Aldrich, Budapest, Hungary) were added 15 min prior to the addition of the antifungal protein. Hyphal growth was determined by measuring the optical density at 620 nm in 96-well flat-bottom microplates (Greiner, Kremsmuenster, Austria) with a microtiter plate reader 340 ATC (SLT Lab Instruments, Groeding, Austria).

Potentiometric staining. The effect of PAF on the membrane potential of *A. nidulans* was monitored by potentiometric staining with the fluorescent dye di-8-ANEPPS (Molecular Probes, Eugene, Oreg.). Fungal conidia (10^3 to 10^4/ml) were grown overnight in YPD medium on coverslips and washed in 2% glucose–16 mM glutamine (GG-solution) before loading with a 12 μM concentration of the dye and 0.1% Pluronic F-127 detergent (Molecular Probes) in GG-solution for 20 min. Subsequently, the dye was washed away, and the specimens were treated with 0 to 10 μg of PAF/ml in GG-solution for 80 min. During this time the coverslips had been mounted on the microscope chamber, and changes in fluorescence staining and intensity were monitored with a laser scanning microscope LSM 510 (Zeiss, Jena, Germany), recording fluorescence intensities excited at 488 nm and detecting emission at 560 nm (F_{560}) by using an interference filter and above 620 nm (F_{620}) by using a high-pass filter. Images were processed with the Zeiss LSM software 5.0 version or by self-written programs. The recorded images were first masked by manually selecting regions of interests (ROIs) and then the ratio ($R = F_{620}/F_{560}$) images were calculated by dividing the corresponding pixels in the ROIs. In this representation, greater R values correspond to larger negative potentials (5). Differences in potential-dependent fluorescence emission ratios (ΔR) were calculated from signals in the first hyphal segments between the hyphal tip and the area adjacent to the first septum.

Staining with fluorescent dyes. PS externalization and DNA fragmentation were tested on protoplasts. Mycelium was harvested on sintered glass and washed with 0.6 M $MgSO_4$ before protoplasts were prepared according to the method of Vagvolgyi and Ferenczy (72). A total of 4×10^6 protoplasts were resuspended in 100 μl of isotonic solution (1 M sorbitol, 10 mM Tris-HCl [pH 7.5]) and were treated with 50 μg of PAF/ml. PS exposure on the protoplast surface was determined after 1 and 3 h of PAF treatment by Annexin V assay using Vybrant Apoptosis Assay Kit #2 (Molecular Probes) according to the manufacturer's instructions. To identify cells undergoing DNA fragmentation, protoplasts, which were treated for 1 h and 3 h with PAF, were subjected to TUNEL (terminal deoxynucleotidyltransferase-mediated dUTP-biotin nick end labeling) by using the APO-BrdU TUNEL Assay Kit (Molecular Probes) according to the manufacturer's instructions. Necrotic cells were detected by propidium iodide (PI) staining. DAPI (4′,6′-diamidino-2-phenylindole) staining was used to determine nuclei-containing protoplasts as described previously (51). In all staining assays, 5,000 protoplasts were analyzed at each incubation time tested.

To detect the formation of ROS, PAF-treated hyphae were incubated in 100 μl of dichlorodihydrofluorescein diacetate (H_2DCFDA; Molecular Probes) at a concentration of 10 μM in phosphate-buffered saline as described by Ezaki et al. (22). As a control for ROS formation, hyphae treated with 5 μg of nystatin/ml (hyphal wet weight) were used.

Stained hyphal specimens were visualized by fluorescence microscopy with a Zeiss (Jena, Germany) Axioplan fluorescence microscope or an LSM 510 laser scanning microscope (Zeiss), with appropriate filters: excitation/emission at 488/530 nm for green fluorescent Alexa Fluor Annexin V, Alexa Fluor 488 dye-labeled anti-BrdU antibody, and H_2DCFDA; excitation/emission at 530/590 nm for red fluorescent PI; and excitation/emission at 365/450 nm for blue fluorescent DAPI.

Ultrastructural analysis. For transmission electron microscopy (TEM), 10^6 conidia were seeded in 1 ml of YPD in 24-well plates (TPP). After 24 h of incubation at 30°C, hyphae were exposed to 50 μg of PAF/ml for 3 h at room temperature. Untreated hyphae were used as a control. Specimens were fixed with 2.5% glutaraldehyde in cacodylate buffer (CCB [vol/vol]; 21.4 g of sodium cacodylate × $3H_2O$/liter [pH 7.3]) for 1 h at 4°C. After a wash with CCB for 10 min at room temperature, specimens were postfixed in reduced osmium tetroxide (0.5% OsO_4 and 0.75% potassium ferrocyanide in CCB) for 1 h at room temperature. After three wash steps (10 min each) mycelia were dehydrated in standard ethanol series and embedded in Spurr's low-viscosity resin (Plano, Marburg, Germany) for 18 h at 4°C. Semithin (300 nm), and ultrathin sections (50 to 90 nm) were cut with a Leica Ultracut UCT (Leica, Vienna, Austria), mounted on regular hexagonal copper grids, double stained with uranyl acetate and lead citrate, and examined with a Zeiss 902 transmission electron microscope.

Statistics. All statistics were done with the Microsoft Excel program. Unless otherwise stated, the standard deviation was <10% in all experiments.

RESULTS

Heterotrimeric G-protein signaling is involved in PAF toxicity. The *flbA* and *fadA* genes encode a regulator of G-protein signaling (RGS) and a heterotrimeric G-protein α-subunit, respectively. Both genes control the balance between cell growth and sporulation in *A. nidulans*. Δ*flbA* enhances intrinsic GTPase activity of Gα subunits, which results in a negative control of intracellular signaling, and Δ*flbA* mutants have been described to show "fluffy autolysis" phenotypes because they fail to make the transition from vegetative growth to conidiogenesis (40, 74, 76). The *fadA*^{G203R} mutation occurs in the guanidine nucleotide binding domain of FadA and affects the ability of the Gα subunit to dissociate from Gβγ, which results in constitutive inactivation of heterotrimeric G-protein signaling and in reduced growth and intensive sporulation (76).

Growth activity assays revealed that the dominant-interfer-

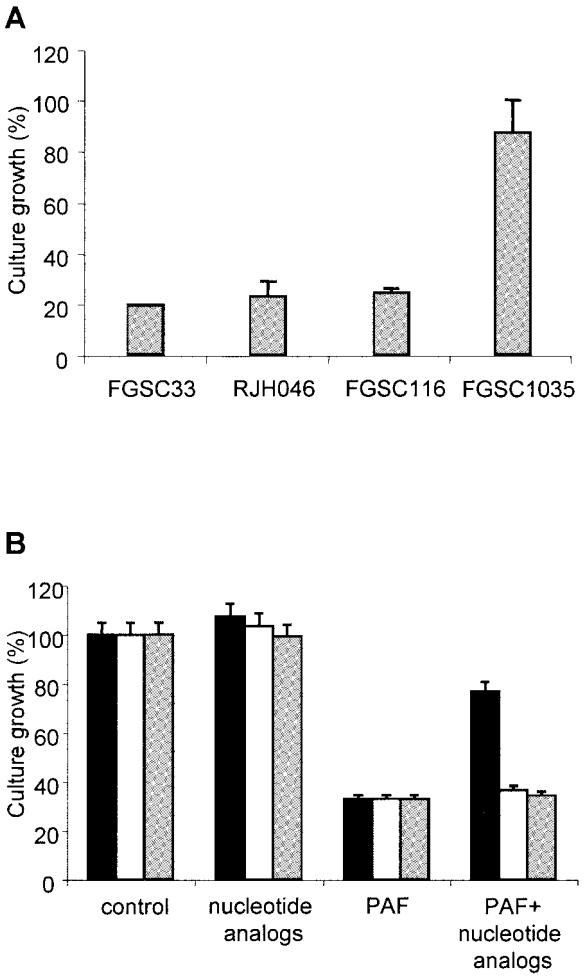

FIG. 1. Effect of mutations affecting G-protein signaling in *A. nidulans*. (A) Conidia of the strains FGSC33, RJH046 (Δ*flbA*), FGSC116, and FGSC1035 (*fadA*^{G203R}) were treated with 10 μg of PAF/ml for 48 h at room temperature. (B) Fungal hyphae were pretreated with 100 μM concentrations of the nucleotide analogs GTPγS (■), GDPβS (□), and ATPγS (▨) before 10 μg of PAF/ml was added, followed by incubation for 24 h at room temperature. Values represent the growth percentage of the tested strains compared to the untreated control (i.e., 100%). Samples were prepared in triplicates.

ing *fadA*^{G203R} mutation confers resistance to PAF in the *A. nidulans* strain FGSC1035 (Fig. 1A). In contrast, deletion of *flbA* could not save the strain RJH046 from PAF-mediated cytotoxicity (Fig. 1A) and sensitivity to PAF was comparable to that of the wt strain and the parental strains FGSC116 and FGSC33, the latter two serving as isogenic controls for FGSC1035 and RJH046, respectively (Fig. 1A). These results indicate that toxicity of PAF is connected to intracellular G-protein signaling.

However, inconsistent results were obtained in the presence of the guanidine nucleotide analogs GTPγS and GDPβS, which both affect G-protein signaling by locking G-proteins in a GTP-bound active form and in a GDP-bound inactive form, respectively (24, 33). *A. nidulans* was less sensitive to PAF treatment in the presence of 100 μM GTPγS, which stimulates G-protein signaling, than in the absence of the nucleotide analog (Fig. 1B). In contrast, GDPβS, which blocks G-protein signaling, was not able to neutralize the effect of PAF. The addition of ATPγS, a nucleotide analog that does not affect G-proteins, showed no significant influence on PAF-induced growth retardation (Fig. 1B).

PAF induces hyperpolarization of the fungal membranes. To establish whether the previously observed potassium efflux after PAF treatment (32) is due to nonspecific membrane damage or to the activation of a K^+ specific pathway, changes in the membrane potential of PAF treated *A. nidulans* were measured. Although a nonspecific increase in membrane permeability should result in a depolarization, a K^+ selective increase in permeability should lead to the hyperpolarization of the fungal membrane, which becomes evident as a shift toward more negative membrane potentials.

Changes in the membrane potential of *A. nidulans* hyphae due to PAF treatment were thus monitored by using the styryl dye di-8-ANEPPS, which is nonfluorescent in aqueous solution and exhibits characteristic absorption/emission maxima of 480/600 nm when bound to phospholipid moieties of cellular membranes. Untreated fungal hyphae accumulated the styryl dye predominantly in the cytoplasmic membrane and to a lesser extent in subcellular membranous structures, which are visible as undefined fluorescent patches within the cytoplasm in Fig. 2A to C. Untreated fungi had characteristically greater ratios

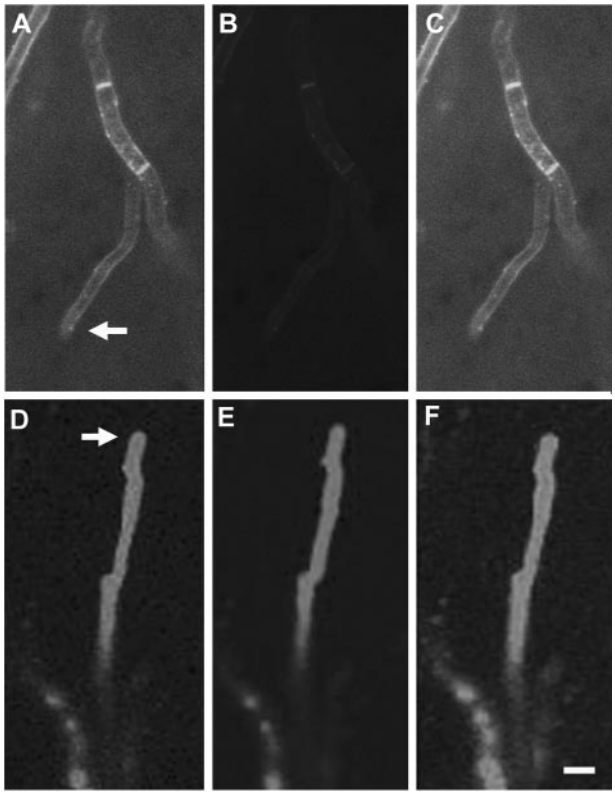

FIG. 2. Potentiometric fluorescence staining of *A. nidulans* wt hyphae with di-8-ANEPPS. (A to C) The plasma membrane of *A. nidulans* was loaded with di-8-ANEPPS for 20 min prior to PAF addition. (D to F) Hyperpolarization of the cellular membranes reached its maximum after 80 min of incubation with 10 μg of PAF/ml at room temperature. The fluorescence was recorded at 560 nm (A and D) and at 620 nm (B and E) and micrographs were merged (C and F). Arrows indicate hyphal tips. Scale bar, 5 μm.

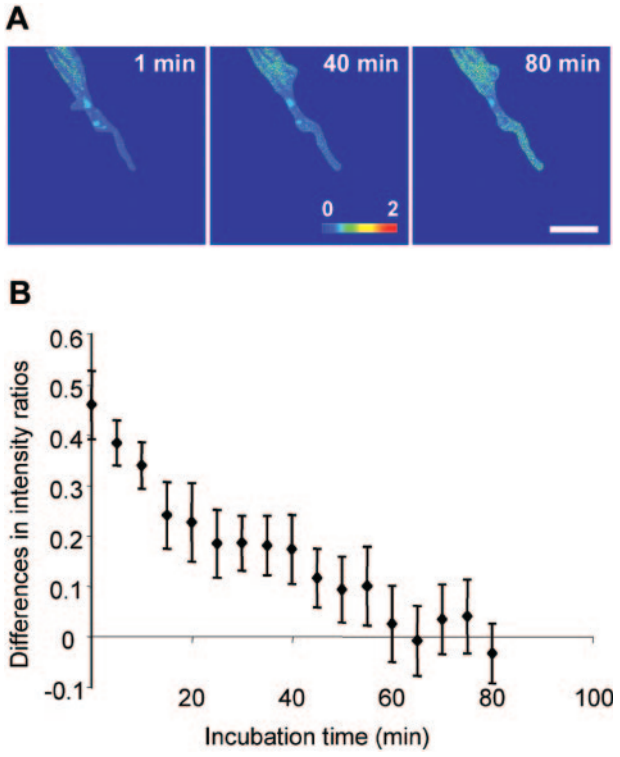

FIG. 3. Fluorescence intensity difference of di-8-ANEPPS labeled and PAF-treated *A. nidulans* wt hyphae as a function of incubation time. (A) Hyperpolarization of the cellular membranes, as assessed by calculating the ratios of images representing ROIs, reached its maximum after 80 min of incubation with 10 μg of PAF/ml at room temperature. Ratio images were obtained at 1, 40, and 80 min after the addition of PAF. (B) Differences in intensity ratios of F_{620}/F_{560} determined near the first septum and at the hyphal tip over the 80 min of incubation with 10 μg of PAF/ml at room temperature. The results are expressed as mean ± the standard deviation ($n = 3$). Scale bar, 25 μm.

($R = F_{620}/F_{560}$), corresponding to more negative membrane potentials, in the first hyphal segments near the first septa (0.79 ± 0.21, $n = 27$) than at the hyphal tips (0.47 ± 0.10, $n = 27$). In the first image of Fig. 3A this is apparent as more green pixels in the first segment near the septum compared to the tip. This difference in R values (ΔR; calculated as R at the first segment minus R at the tip) was present for all fungal hyphae, indicating that hyphal tips are depolarized compared to the regions near the first septa under untreated conditions. The addition of 10 μg of PAF/ml immediately induced a time-dependent increase in signal intensity in the first hyphal segments. The fluorescence signal spread from the hyphal tips and proceeded along to the adjacent areas near the septa. In parallel, the ratio of the fluorescence intensities increased, a finding indicative of an overall hyperpolarization of the fungal membranes (Fig. 2D to F and Fig. 3A; note the appearance of more green and yellow pixels in the last two images of Fig. 3A). Similar events took place at the hyphal tips as well, although the changes were more pronounced than in the adjacent regions, i.e., the hyperpolarization was more prominent at the tips than near the first septa. This led to a decrease in ΔR, that is, in the difference between the ratio values in the first hyphal segment near the septum and in the hyphal tip (Fig. 3). At 80 min after the addition of PAF, ΔR was essentially zero, indicating that there was no longer any potential difference along the hyphae (Fig. 3B). PAF-untreated hyphae that were observed during the same time period exhibited neither changes in fluorescence signal distribution nor changes in fluorescence ratios with $\Delta R = 0.4 \pm 0.13$ ($n = 3$) at the start and with $\Delta R = 0.4 \pm 0.06$ ($n = 3$) after 80 min, respectively (data not shown).

PAF induces intracellular ROS. Elevated levels of intracellular ROS is a major elicitor of PCD. We could previously show the generation of intracellular ROS in PAF-treated *A. niger* hyphae and the ROS-induced modification of proteins in the cellular extracts of *A. nidulans*, expressing recombinant PAF (32, 48). In order to investigate the site of ROS formation in *A. nidulans*, PAF-treated hyphae were labeled with H_2DCFDA (Fig. 4A). The ROS-specific signals were distributed along the plasma membrane and within the cytoplasm (Fig. 4A) and resembled the signal induced with 5 μg of nystatin/ml (hyphal wet weight) (Fig. 4B), which is known to trigger ROS production by the oxidation of the phospholipid moieties of cellular membranes (50). No ROS specific signals were detected in untreated hyphae (Fig. 4C and D).

PAF-treated fungal cells expose PS on their surface and are TUNEL positive. PS exposure on the surface of cells and DNA strand breaks are universal phenomena during apoptosis that occur in most cell types and organisms in response to diverse cell death signals (16, 51, 53, 73). We tested *A. nidulans* protoplasts that were either left untreated (control) or exposed to

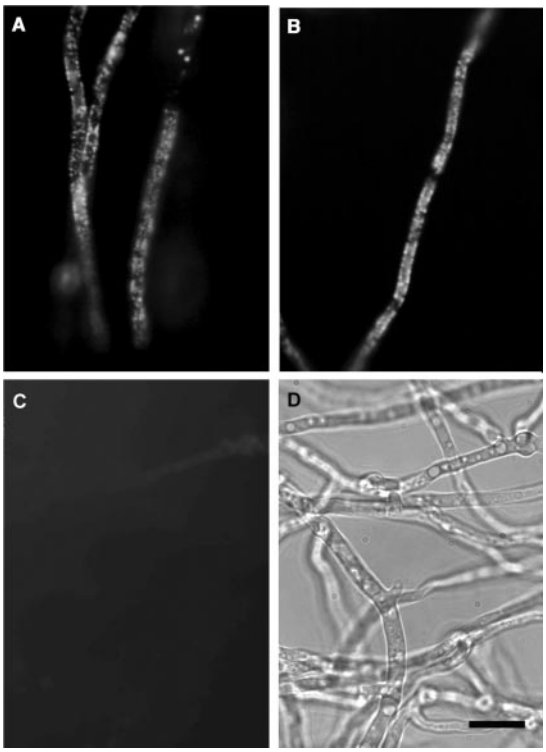

FIG. 4. Detection of intracellular ROS by H_2DCFDA in *A. nidulans* wt. (A and B) Hyphae were treated with 50 μg of PAF/ml for 90 min at room temperature (A) or with 5 μg of nystatin/mg (hyphal wet weight) as a control for ROS generation (B) before labeling with H_2DCFDA. (C) Untreated control labeled with H_2DCFDA. (D) Phase contrast of image in panel C. Scale bar, 10 μm.

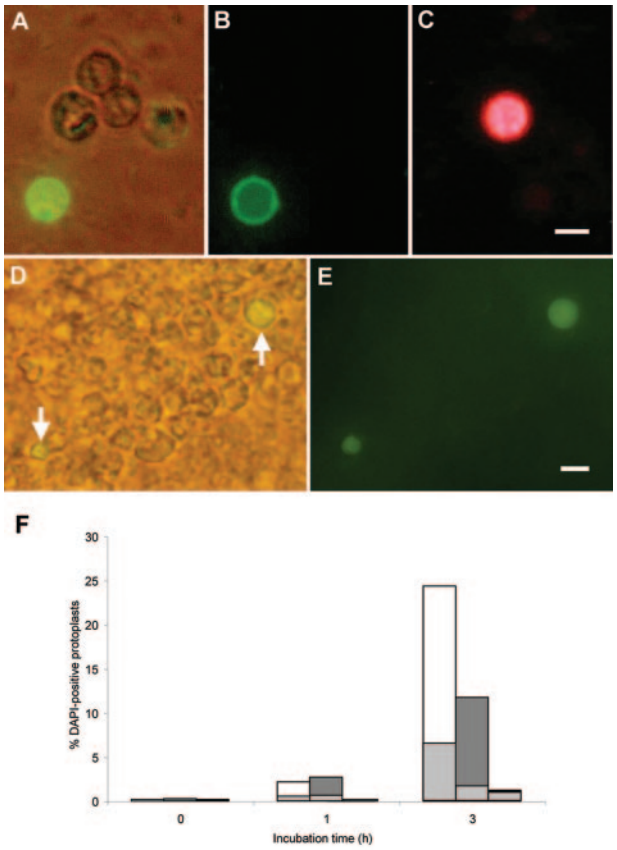

FIG. 5. Detection of apoptotic markers in *A. nidulans* protoplasts after treatment with 50 μg of PAF/ml. Annexin V (A and B)- and PI (C)-stained protoplasts after PAF exposure for 3 h and TUNEL-stained nuclei in protoplasts after incubation for 1 h (D and E) were visualized by microscopy by using phase contrast and fluorescence (A and D) and fluorescence alone (B, C, and E), respectively. Two TUNEL-positive cells are indicated by arrows in panel D. Scale bars, 5 μm. (F) Results are shown as the percentage of DAPI-positive protoplasts that stain positive with Annexin V (white), TUNEL (dark gray), or PI (black) at time zero and after 1 and 3 h of incubation with PAF. Light gray portions indicate the percentage of positively stained protoplasts without PAF treatment.

50 μg of PAF/ml for various periods of time. The flip-flop of PS from the inner to the outer plasma membrane was monitored by using Annexin V staining (Fig. 5A and B), and DNA fragmentation was visualized by the TUNEL method (Fig. 5D and E). Annexin V has a high affinity for PS (78). Therefore, apoptotic cells showed green fluorescence due to PS exposure on the outer leaflet, whereas viable cells had little or no fluorescence (Fig. 5A and B). Less than 0.2% of DAPI-positive protoplasts were Annexin V positive at time point zero of the PAF treatment experiment. The percentage of apoptotic cells increased by the addition of PAF to ~2.2% after 1 h of incubation versus ~0.5% in the PAF-untreated control and proceeded to ca. 24.4% after 3 h of incubation versus ~6.1% in the control (Fig. 5F). Thus, the generation of protoplasts per se induced an increase of Annexin V-positive cells with the time. However, a fourfold-higher percentage of protoplasts exhibiting PS externalization after 3 h of incubation in the presence of PAF compared to the control points to a protein-specific induction.

Another landmark of apoptosis is DNA fragmentation due to the cleavage of linker regions between nucleosomes by nucleases (2, 23). The labeling of DNA breaks by TUNEL is one of the most reliable methods for the identification of apoptotic cells (7). Indeed, staining of 3′-OH ends of DNA breaks in *A. nidulans* protoplasts, which were treated with 50 μg of PAF/ml, revealed an increase in TUNEL-positive cells compared to the untreated control (Fig. 5D and E). Similar to the Annexin V membrane inversion assay, the percentage of TUNEL-positive, nuclei-containing cells at time point zero was <0.3% and increased to ~2.7% after 1 h and to ~11.7% after 3 h of PAF treatment versus <0.6% after 1 h and ~1.6% after 3 h in the controls, respectively (Fig. 5F).

Finally, necrosis was visualized by staining the protoplasts with PI, which tightly binds to nucleic acids and is permeant only to necrotic cells (3) (Fig. 5C). The number of DAPI-positive necrotic cells did not differ significantly between PAF-treated and untreated protoplasts, although also in this case the number of necrotic protoplasts increased with the incubation time: <0.2% after 1 h and <1.2% after 3 h of incubation in the presence of PAF versus <0.2% after 1 h and <1.0% after 3 h of incubation in control cultures (Fig. 5F).

PAF activity results in the disintegration of subcellular structures. Further tests of apoptotic markers were performed by examining the ultrastructure of fungal hyphae in ultrathin sections by TEM (Fig. 6). Untreated *A. nidulans* hyphae featured cells with regular submicroscopic structure and clearly identifiable organelles (Fig. 6A to C). Hyphal segments typically contained several nuclei surrounded by the nuclear membrane and nucleoli were visible in many cases (Fig. 6A and C). The numerous mitochondria with membranous cristae always showed well-preserved outer and inner membranes. Vacuoles were small and empty or contained loosely distributed material (Fig. 6A and B). The fungal cytoplasmic membrane was visible as a sharp, electron-dense lipid bilayer, surrounded by the cell wall that appeared as a dark inner, finely granular layer and a bright outer fibrous layer (Fig. 6B and C).

Compared to the untreated cells, the PAF-treated hyphae showed an abnormal subcellular morphology (Fig. 6D to F). The cell wall had lost its granularity and its architecture. The shrunk cytoplasm detached from the cell wall and microvesicle-like structures had formed between the cell wall and the cell membrane (Fig. 6E and F). In the cytoplasm, mitochondria were less well defined and often displayed discontinuous or missing outer membranes. The nuclear membrane disappeared (Fig. 6D). Large vacuoles became apparent (Fig. 6E). With progressing cell injury, no distinct cytoplasmic organelles were detectable, and the whole cell had disintegrated. These features appeared frequently, but not all of them occurred in every cell.

DISCUSSION

We investigated here the role of heterotrimeric G-protein signaling in PAF-toxicity. Previous reports suggested that the cytotoxicity of antifungal proteins could involve the interference with G-protein signaling (19, 70, 77). Nevertheless, the reported findings are controversial, and the way antifungal activity is connected to G-protein signaling seems to strongly depend on the antifungal peptides tested. Indeed, we could confirm a G-protein-related activity of PAF in *A. nidulans* by

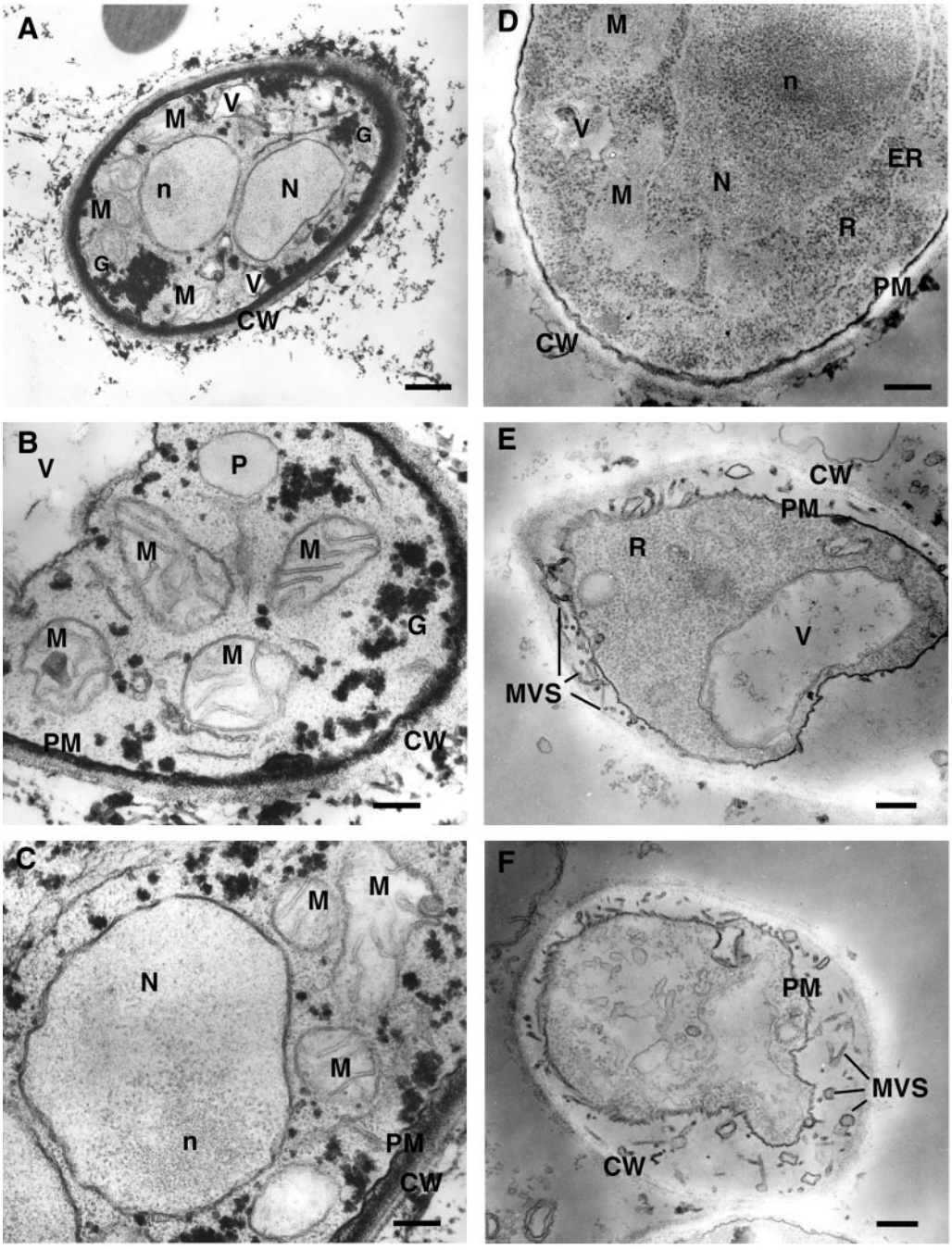

FIG. 6. TEM images of the cellular ultrastucture of *A. nidulans*. (A to C) Untreated control; (D to F) specimens were treated with 50 μg of PAF/ml for 3 h at room temperature. CW, cell wall; ER, endoplasmic reticulum; G, glycogen; M, mitochondrion; MVS, microvesicular structures; N, nucleus; n, nucleolus; P, peroxisome; PM, plasma membrane; R, ribosomes; V, vacuole. Scale bars: 0.25 μm (A, B, C, E, and F) and 0.6 μm (D).

using G-protein mutants. The growth inhibition caused by PAF presumed active heterotrimeric G-protein signaling which was indicated by the reduction of PAF sensitivity of the dominant-interfering $fadA^{G203R}$ mutant FGSC1035. This result parallels the reported osmotin resistance of the interfering $fadA^{G203R}$ mutation in the *A. nidulans* strain TJY115.4 (19).

The finding that the Δ*flbA* mutant strain RJH046 was similarly affected by PAF as the parental strain FGSC33 supports the hypothesis that PAF needs active G-protein signaling to inhibit the growth of the sensitive organism. This finding is in contrast to the observed osmotin resistance of the *A. nidulans* Δ*flbA* mutant strain TNB39.5 (19) but agrees with findings in *Saccharomyces cerevisiae*, where inactivation of the *flbA* paralogous gene *sst2* could not prevent sensitivity to osmotin (77). The fact that the nucleotide analog GTPγS, but not GDPβS, negatively affected PAF activity was unexpected because this observation did not match the results gained with the $fadA^{G203R}$ and Δ*flbA* mutants. However, one has to consider

that nucleotide analogs may interact with various GTP-binding proteins other than the RGS-Gα pair FlbA and FadA, e.g., the Gα subunits GanA and GanB or the RGS protein RgsA (15, 29), or with monomeric G proteins, i.e., Rho, Ras, and Cdc42 (9, 28, 30, 66), all of which interact with various effector molecules and are intimately involved in diverse physiological functions (1, 11, 36, 54). Therefore, G-protein inhibition studies with GTPγS and GDPβS reflect the response of a complex network of monomeric and heterotrimeric G-proteins to PAF in a wild-type strain and not solely that of the FadA/FlbA system.

Based on our previous findings of an active internalization of PAF into hyphae of sensitive fungi (55), PAF could either interact directly with one of the G-protein subunits—analogous to other toxins (39, 58)—or trigger indirectly a G-protein-based signal. Alternatively, PAF toxicity may be dependent on the physiological state of the target organism, which is strongly regulated by the concerted action of the different G proteins (1, 49). However, at present we are not able to discriminate between a direct and an indirect role of FadA-dependent heterotrimeric G-protein signaling in the toxicity of PAF, and thus further analysis of PAF-elicited responses in various *A. nidulans* G-protein mutants is necessary to understand the signaling mechanism.

Importantly, G-protein signaling could mediate PCD. In contrast to the monomeric G-protein signaling, whose fundamental role in the regulation of apoptosis is well established in higher and lower eukaryotes (53, 65, 80), the role of heterotrimeric G-protein signaling in the induction of apoptosis has been implicated only recently for higher eukaryotes (36, 60). Thus far, the pathways involved are still poorly understood, and no evidence has been presented for yeasts or filamentous fungi. However, heterotrimeric G-protein signaling is well known to regulate second messenger levels (e.g., cyclic AMP) and ion channels (18), which could directly account for the PAF-dependent hyperpolarization of plasma membranes and for the apoptosis-like phenotype described in the present study.

As a consequence of the interaction of PAF with the sensitive mold *A. nidulans*, the hyperpolarization of the plasma membrane is evoked. The membrane potential in fungi is maintained by active H^+ ion extrusion (61), and it is likely that PAF directly or indirectly interacts with the plasma membrane H^+ pump or, alternatively, it triggers ion effluxes. Indeed, a significantly elevated K^+ efflux in PAF-treated *A. nidulans* hyphae has been reported previously by Kaiserer et al. (32) and is in good agreement with the membrane hyperpolarization reported here. Both observations point to the activation of specific ion, most likely potassium, channels. These mechanisms are different from those reported on antimicrobial proteins from bacteria, insects, and humans, which form voltage-gated ion channels with little species specificity in the membranes of target organisms and which exhibit increased biological activity at higher temperatures (8, 20, 31). This is due to the fact that membrane fluidity is enhanced at higher temperatures and therefore facilitates protein insertion. There are several observations that make plasma membrane permeabilization by PAF via nonspecific pore formation rather unlikely: PAF (i) activates ion channels; (ii) acts only on filamentous fungi; (iii) is actively internalized; and (iv) is equally active at temperatures between 25 and 30°C, whereby its activity slowly declines with higher temperatures (unpublished data). These findings support our assumption that PAF activity is mediated by a specific receptor, which has also been suggested for several plant defensins that show a similar temperature-independent activity (56, 70). However, no specific receptor has been identified thus far, although such a target for antifungal proteins would provide us with important information about the mechanism of their action.

The hyperpolarization of cellular membranes starts immediately after PAF addition and precedes the appearance of other apoptotic markers. This is similar to mammalian cells, in which membrane hyperpolarization and K^+ efflux mediate further apoptotic events (59, 79, 81). Indeed, the intracellular accumulation of ROS is one of the major stimuli for the induction of PCD found in lower and higher eukaryotes (27, 41, 43, 52, 65, 80). Actually, we demonstrated the PAF-dependent generation of ROS in *A. nidulans*. The same was previously observed to occur in *A. niger* hyphae (32) and, hence, the onset of oxidative stress seems to be common in PAF-treated sensitive fungi. In general, mitochondria are the main sources of ROS in aerobic microorganisms and are prone to oxidative injuries and even disintegration, when the imbalance between ROS production and elimination becomes long-lasting (13, 14, 57, 62, 63, 64). This can ultimately result in the aggravation of the ROS burden for the cell and the release of apoptosis-inducing proteins, such as cytochrome *c*, apoptosis inducing factor, and metacaspases and caspases, which have also been detected in *S. cerevisiae* (38) and in *A. nidulans* (16, 71). Indeed, an aberrant ultrastructural morphology of mitochondria in *A. nidulans* hyphae became evident after PAF treatment, indicating mitoptosis and malfunction of these organelles.

Further evidence for an apoptosis-like cell death mechanism induced by PAF is given by an increase in the number of protoplasts positively stained in both Annexin V and TUNEL labelings. The translocation of PS from the inner to the outer leaflet of the plasma membrane and DNA fragmentation occur not only in mammalian cells but are also found in yeasts and in filamentous fungi and underline similarities in apoptotic cell death (16, 38, 44, 51). Furthermore, the lower percentage of TUNEL-positive *A. nidulans* protoplasts after PAF exposure parallels observations made with phytosphingosine-treated *A. nidulans* cells (16) and indicates that PS translocation preceded DNA fragmentation.

Finally, the detection of additional ultrastructural changes due to PAF treatment substantiates the occurrence of an apoptosis-like mechanism: the detachment of the plasma membrane from the cell wall, the appearance of microvesicles, and cytoplasmic shrinkage. The formation of microvesicles between the plasma membrane and the cell wall of PAF-treated hyphae resembles membrane blebbing, a major characteristic of apoptotic cells (34). Similar effects were also reported to be induced by cell wall-active agents, which are promising candidates for antimycotic treatment, e.g., the glucan synthase inhibitor echinocandin and the chitin synthase inhibitor nikkomycin (17). Both apoptotic and necrotic cell death are associated with the impairment or alteration of cell volume regulation but, in contrast to necrotic cell death, cell shrinkage is a typical feature of PCD (25, 34, 75).

Although the PAF-induced growth inhibition in *A. nidulans*

revealed numerous markers of apoptosis, it has to be taken into account that necrosis may also be triggered and may be progressing, too. Apoptosis and necrosis can occur in the same cell population and are thought to be elicited by the same signals; thus, the choice between these two outcomes is cell specific and depends on various endogenous factors, e.g., the cellular ATP level or the activation of proapoptotic proteins (26). Protoplasts from filamentous fungi derive from hyphal segments of very diverse physiological and developmental stages. This explains why both events can be found in PAF-treated cells. Importantly, the percentage of necrotic protoplasts in PAF-treated samples was comparable to that recorded for the controls, indicating that the cell death process evoked by PAF clearly resembled an apoptotic event.

Further investigations of the role of the multiple effects triggered by PAF are needed to elucidate the exact mechanism leading to an apoptosis-like phenotype in sensitive fungi. The data presented here and our recent findings that various mammalian cells, including neurons, astrocytes, skeletal muscle fibers, and endothelial cells from the umbilical vein, remain unaffected by PAF and that PAF also did not induce the production of proinflammatory cytokines (e.g., interleukin-6, interleukin-8, and tumor necrosis factor alpha) (67) indicate that this protein is a promising candidate for the development of new antifungal drugs.

ACKNOWLEDGMENTS

We thank Renate Weiler-Görz for assistance with PAF purification and Hubertus Haas for helpful discussions.

This study was funded by the Austrian Science Foundation (grant FWF P15261), the Austrian National Bank (grant ÖNB 9861), the University of Innsbruck (grants X8 and X34), the Hungarian Scientific Research Fund (grants D034568, T034315, T037473, and T034894), and the Hungarian Office for Higher Education Programs (grant 0092/2001). The Hungarian Ministry of Education awarded a Szechenyi Istvan Scholarship to I.P.

REFERENCES

1. **Adams, T. H., J. Wieser, and J.-H. Yu.** 1998. Asexual sporulation in *Aspergillus nidulans*. Microbiol. Mol. Biol. Rev. **62:**35–54.
2. **Arends, M. J., R. G. Morris, and A. H. Wyllie.** 1990. Apoptosis: the role of the endonuclease. Am. J. Pathol. **136:**593–608.
3. **Arndt-Jovin, D. J., and T. M. Jovin.** 1989. Fluorescence labeling and microscopy of DNA. Methods Cell Biol. **30:**417–448.
4. **Barratt, R. W., G. B. Johnson, and W. N. Ogata.** 1965. Wild-type and mutant stocks of *Aspergillus nidulans*. Genetics **52:**233–246.
5. **Beach, J. M., E. D. McGahren, J. Xia, and B. R. Duling.** 1996. Ratiometric measurement of endothelial depolarization in arterioles with a potential-sensitive dye. Am. J. Physiol. **270:**2216–2227.
6. **Borgia, P. T., C. L. Dodge, L. E. Eagleton, and T. H. Adams.** 1994. Bidirectional gene transfer between *Aspergillus fumigatus* and *Aspergillus nidulans*. FEMS Microbiol. Lett. **122:**227–231.
7. **Bortner, C. D., N. B. E. Oldenburg, and J. A. Cidlowski.** 1995. The role of DNA fragmentation in apoptosis. Trends Cell Biol. **5:**21–26.
8. **Bourdineaud, J. P., P. Boulanger, C. Lazdunski, and L. Letellier.** 1990. In vivo properties of colicin A: channel activity is voltage dependent but translocation may be voltage independent. Proc. Natl. Acad. Sci. USA **87:**1037–1041.
9. **Boyce, K. J., M. J. Hynes, and A. Andrianopoulos.** 2001. The CDC42 homolog of the dimorphic fungus *Penicillium marneffei* is required for correct cell polarization during growth but not development. J. Bacteriol. **183:**2447–2457.
10. **Broekaert, W. F., F. R. G. Terras, B. P. A. Cammue, and J. Vanderleyden.** 1990. An automated quantitative assay for fungal growth inhibition. FEMS Microbiol. Lett. **69:**55–59.
11. **Burchett, S. A.** 2000. Regulators of G protein signaling: a bestiary of modular protein binding domains. J. Neurochem. **75:**1335–1351.
12. **Cabiscol, E., E. Piulats, P. Echave, E. Herrero, and J. Ros.** 2000. Oxidative stress promotes specific protein damage in *Saccharomyces cerevisiae*. J. Biol. Chem. **275:**27393–27398.
13. **Camougrand, N., I. Kissová, G. Velours, and S. Manon.** 2004. Uth1p: a yeast mitochondrial protein at the crossroads of stress, degradation and cell death. FEMS Yeast Res. **5:**133–140.
14. **Cardomy, R. J., and T. G. Cotter.** 2001. Signalling apoptosis: a radical approach. Redox Rep. **6:**77–90.
15. **Chang, M. H., K.-S. Chae, D.-M. Han, and K.-W. Jahng.** 2004. The GanB Gα protein negatively regulates asexual sporulation and plays a positive role in conidial germination in *Aspergillus nidulans*. Genetics **167:**1305–1315.
16. **Cheng, J., T.-S. Park, L.-C. Chio, A. S. Fischl, and X. S. Ye.** 2003. Induction of apoptosis by sphingoid long-chain bases in *Aspergillus nidulans*. Mol. Cell. Biol. **23:**163–177.
17. **Chiou, C. C., N. Mavrogiorgos, E. Tillem, R. Hector, and T. J. Walsh.** 2001. Synergy, pharmacodynamics, and time-sequenced ultrastructural changes of the interaction between nikkomycin Z and the echinocandin FK463 against *Aspergillus fumigatus*. Antimicrob. Agents Chemother. **45:**3310–3321.
18. **Clapham, D. E., and E. J. Neer.** 1993. New roles for G protein by dimers in transmembrane signaling. Nature **265:**403–406.
19. **Coca, M. A., B. Damsz, D. J. Yun, P. M. Hasegawa, R. A. Bressan, and M. L. Narasimhan.** 2000. Heterotrimeric G-proteins of a filamentous fungus regulate cell wall composition and susceptibility to a plant PR-5 protein. Plant J. **22:**61–69.
20. **Cociancich, S., A. Ghazi, C. Hetru, J. A. Hoffmann, and L. Letellier.** 1993. Insect defensin, an inducible antibacterial peptide, forms voltage-dependent channels in *Micrococcus luteus*. J. Biol. Chem. **268:**19239–19245.
21. **Denning, D. W., M. J. Anderson, G. Turner, J. P. Latge, and J. W. Bennett.** 2002. Sequencing the *Aspergillus fumigatus* genome. Lancet Infect. Dis. **2:**251–253.
22. **Ezaki, B., R. C. Gardner, Y. Ezaki, and H. Matsumoto.** 2000. Expression of aluminium-induced genes in transgenic *Arabidopsis* plants can ameliorate aluminium stress and/or oxidative stress. Plant Physiol. **122:**657–665.
23. **Gavrieli, Y., Y. Sherman, and S. A. Ben-Sasson.** 1992. Identification of programmed cell death in situ via specific labeling of nuclear DNA fragmentation. J. Cell Biol. **119:**493–501.
24. **Gilman, A. G.** 1987. G proteins: transducers of receptor-generated signals. Annu. Rev. Biochem. **56:**615–649.
25. **Gomez-Angelats, M., C. D. Bortner, and J. A. Cidlowski.** 2000. Cell volume regulation in immune cell apoptosis. Cell Tissue Res. **301:**33–42.
26. **Green, D. R., and J. C. Reed.** 1998. Mitochondria and apoptosis. Science **281:**1309–1312.
27. **Greenlund, L. J., T. L. Deckwerth, and E. M. Johnson.** 1995. Superoxide dismutase delays neuronal apoptosis: a role for reactive oxygen species in programmed neuronal death. Neuron **14:**303–315.
28. **Guest, G. M., X. Lin, and M. Momany.** 2004. *Aspergillus nidulans* RhoA is involved in polar growth, branching, and cell wall synthesis. Fungal Genet. Biol. **41:**13–22.
29. **Han, K.-H., J.-A. Seo, and J.-H. Yu.** 2004. Regulators of G-protein signalling in *Aspergillus nidulans*: RgsA downregulates stress response and stimulates asexual sporulation through attenuation of GanB (Gα) signalling. Mol. Microbiol. **53:**529–540.
30. **Hlavata, L., and T. Nystrom.** 2003. Ras proteins control mitochondrial biogenesis and function in *Saccharomyces cerevisiae*. Folia Microbiol. **48:**725–730.
31. **Kagan, B. L., M. E. Selsted, T. Ganz, and R. Lehrer.** 1990. Antimicrobial defensin peptides form voltage-dependent ion-permeable channels in planar lipid bilayer membranes. Proc. Natl. Acad. Sci. USA **87:**210–214.
32. **Kaiserer, L., C. Oberparleiter, R. Weiler-Goerz, W. Burgstaller, E. Leiter, and F. Marx.** 2003. Characterization of the *Penicillium chrysogenum* antifungal protein PAF. Arch. Microbiol. **180:**204–210.
33. **Kaziro, Y., H. Itoh, T. Kozasa, M. Nakafuku, and T. Satoh.** 1991. Structure and function of signal-transducing GTP-binding proteins. Annu. Rev. Biochem. **60:**349–400.
34. **Kerr, J. F. R.** 1993. Definition of apoptosis and overview of its incidence, p. 1–18. *In* M. Lavin and D. Watters (ed.), Programmed cell death: the cellular and molecular biology of apoptosis. Harwood Academic Publishers, Amsterdam, The Netherlands.
35. **Klyubin, I. V., K. M. Kirpichnikova, A. M. Ischenko, A. V. Zhakhov, and I. A. Gamaley.** 2000. The role of reactive oxygen species in membrane potential changes in macrophages and astrocytes. Membr. Cell Biol. **13:**557–566.
36. **Kowluru, A., and N. G. Morgan.** 2002. GTP-binding proteins in cell survival and demise: the emerging picture in the pancreatic β-cell. Biochem. Pharmacol. **63:**1027–1035.
37. **Latgé, J. P.** 1999. *Aspergillus fumigatus* and aspergillosis. Clin. Microbiol. Rev. **12:**310–350.
38. **Laun, P., A. Pichova, F. Madeo, J. Fuchs, A. Ellinger, S. Kohlwein, I. Dawes, K. U. Frohlich, and M. Breitenbach.** 2001. Aged mother cells of *Saccharomyces cerevisiae* show markers of oxidative stress and apoptosis. Mol. Microbiol. **39:**1166–1173.
39. **Lax, A. J., G. D. Pullinger, M. R. Baldwin, D. Harmey, A. E. Grigoriadis, and J. H. Lakey.** 2004. The *Pasteurella multocida* toxin interacts with signalling pathways to perturb cell growth and differentiation. Int. J. Med. Microbiol. **293:**505–512.
40. **Lee, B. N., and T. H. Adams.** 1994. Overexpression of *flbA*, an early regulator

of *Aspergillus* asexual sporulation, leads to activation of *brlA* and premature initiation of development. Mol. Microbiol. **14:**323–334.
41. **Ligr, M., F. Madeo, E. Froehlich, W. Hilt, K.-U. Froehlich, and D. H. Wolf.** 1998. Mammalian Bax triggers apoptotic changes in yeast. FEBS Lett. **438:** 61–65.
42. **Ludwig, A., and T. Boller.** 1990. A method for the study of fungal growth inhibition by plant proteins. FEMS Microbiol. Lett. **69:**61–66.
43. **Madeo, F., S. Engelhardt, E. Herker, N. Lehmann, C. Maldener, A. Proksch, S. Wissing, and K.-U. Froehlich.** 2002. Apoptosis in yeast: a new model system with applications in cell biology and medicine. Curr. Genet. **41:** 208–216.
44. **Madeo, F., E. Froehlich, and K.-U. Froehlich.** 1997. A yeast mutant showing diagnostic markers of early and late apoptosis. J. Cell Biol. **139:**729–734.
45. **Madeo, F., E. Froehlich, M. Ligr, M. Grey, S. J. Sigrist, D. H. Wolf, and K.-U. Froehlich.** 1999. Oxygen stress: a regulator of apoptosis in yeast. J. Cell Biol. **145:**757–767.
46. **Marx, F.** 2004. Small, basic antifungal proteins secreted from filamentous ascomycetes: a comparative study regarding expression, structure, function and potential application. Appl. Microbiol. Biotechnol. **65:**133–142.
47. **Marx, F., H. Haas, M. Reindl, G. Stoffler, F. Lottspeich, and B. Redl.** 1995. Cloning, structural organization and regulation of expression of the *Penicillium chrysogenum paf* gene encoding an abundantly secreted protein with antifungal activity. Gene **167:**167–171.
48. **Marx, F., W. Salvenmoser, L. Kaiserer, S. Graessle, R. Weiler-Goerz, I. Zadra, and C. Oberparleiter.** 2005. Proper folding of the antifungal protein PAF is required for optimal activity. Res. Microbiol. **156:**35–46.
49. **Molnar, Z., E. Meszaros, Z. Szilagyi, S. Rosen, T. Emri, and I. Pocsi.** 2004. Influence of fadA^{G203R} and Δ*flbA* mutations on morphology and physiology of submerged *Aspergillus nidulans* cultures. Appl. Biochem. Biotechnol. **118:** 349–360.
50. **Moore, C. B., N. Sayers, J. Mosquera, J. Slaven, and D. W. Denning.** 2000. Antifungal drug resistance in *Aspergillus*. J. Infect. **41:**203–220.
51. **Mousavi, S. A. A., and G. D. Robson.** 2003. Entry into the stationary phase is associated with a rapid loss of viability and an apoptotic-like phenotype in the opportunistic pathogen *Aspergillus fumigatus*. Fungal Genet. Biol. **39:** 221–229.
52. **Mousavi, S. A. A., and G. D. Robson.** 2004. Oxidative and amphotericin B-mediated cell death in the opportunistic pathogen *Aspergillus fumigatus* is associated with an apoptotic-like phenotype. Microbiology **150:**1937–1945.
53. **Narasimhan, M. L., B. Damsz, M. A. Coca, J. I. Ibeas, D.-J. Yun, J. M. Pardo, P. M. Hasegawa, and R. A. Bressan.** 2001. A plant defense response effector induces microbial apoptosis. Mol. Cell **8:**921–930.
54. **Neer, E. J.** 1995. Heterotrimeric G proteins: organizers of transmembrane signals. Cell **80:**249–257.
55. **Oberparleiter, C., L. Kaiserer, H. Haas, P. Ladurner, M. Andratsch, and F. Marx.** 2003. Active internalization of the *Penicillium chrysogenum* antifungal protein PAF in sensitive aspergilli. Antimicrob. Agents Chemother. **47:**3598–3601.
56. **Osborn, R. W., G. W. De Samblanx, K. Thevissen, I. Goderis, S. Torrekens, F. Van Leuven, S. Attenborough, S. B. Rees, and W. F. Broekaert.** 1995. Isolation and characterisation of plant defensins from seeds of *Asteraceae*, *Fabaceae*, *Hippocastanaceae*, and *Saxifragaceae*. FEBS Lett. **368:**257–262.
57. **Osiewacz, H. D.** 2002. Genes, mitochondria and aging in filamentous fungi. Ageing Res. Rev. **1:**425–442.
58. **Pfeuffer, T., and E. J. Helmreich.** 1988. Structural and functional relationships of guanosine triphosphate binding proteins. Curr. Top. Cell Regul. **29:** 129–216.
59. **Remillard, C. V., and J. X. Yuan.** 2004. Activation of K^+ channels: an essential pathway in programmed cell death. Am. J. Physiol. Lung Cell Mol. Physiol. **286:**L49–L67.
60. **Revankar, C. M., C. M. Vines, D. F. Cimino, and E. R. Prossnitz.** 2004. Arrestins block G protein-coupled receptor-mediated apoptosis. J. Biol. Chem. **279:**24578–24584.
61. **Serrano, R., and A. Rodriguez-Navarro.** 2001. Ion homeostasis during salt stress in plants. Curr. Opin. Cell Biol. **13:**399–404.
62. **Singh, K. K.** 2004. Mitochondria damage checkpoint in apoptosis and genome stability. FEMS Yeast Res. **5:**127–132.
63. **Singh, K. K.** 2004. Mitochondrial dysfunction is a common phenotype in aging and cancer. Ann. N. Y. Acad. Sci. **1019:**260–264.
64. **Skulachev, V. P.** 2000. Mitochondria in the programmed death phenomena; a principle of biology: "it is better to die than to be wrong." IUBMB Life **49:** 365–373.
65. **Slater, A. F., C. Stefan, I. Nobel, D. J. van den Dobbelsteen, and S. Orrenius.** 1995. Signalling mechanisms and oxidative stress in apoptosis. Toxicol. Lett. **82–83:**149–153.
66. **Som, T., and V. S. R. Kolaparthi.** 1994. Developmental decisions in *Aspergillus nidulans* are modulated by Ras activity. Mol. Cell. Biol. **14:**5333–5348.
67. **Szappanos, H., G. P. Szigeti, B. Pál, Z. Rusznák, G. Szücs, É. Rajnavölgyi, J. Balla, G. Balla, E. Nagy, É. Leiter, I. Pócsi, F. Marx, and L. Csernoch.** 2005. The *Penicillium chrysogenum*-derived antifungal peptide shows no toxic effects on mammalian cells in the intended therapeutic concentration. Naunyn Schmiedebergs Arch. Pharmacol. **371:**122–132.
68. **Theis, T., F. Marx, W. Salvenmoser, U. Stahl, and V. Meyer.** 2005. New insights into the target site and mode of action of the antifungal protein of *Aspergillus giganteus*. Res. Microbiol. **156:**47–56.
69. **Theis, T., M. Wedde, V. Meyer, and U. Stahl.** 2003. The antifungal protein from *Aspergillus giganteus* causes membrane permeabilization. Antimicrob. Agents Chemother. **47:**588–593.
70. **Thevissen, K., A. Ghazi, G. W. De Samblanx, C. Brownlee, R. W. Osborn, and W. F. Broekaert.** 1996. Fungal membrane responses induced by plant defensins and thionins. J. Biol. Chem. **271:**15018–15025.
71. **Thrane, C., U. Kaufmann, B. M. Stummann, and S. Olsson.** 2004. Activation of caspase-like activity and poly (ADP-ribose) polymerase degradation during sporulation in *Aspergillus nidulans*. Fungal Genet. Biol. **41:**361–368.
72. **Vagvolgyi, C., and L. Ferenczy.** 1991. Isolation of nuclei from *Aspergillus nidulans* protoplasts. FEMS Microbiol. Lett. **66:**247–251.
73. **Vermes, I., C. Haanen, and C. Reutelingsperger.** 2000. Flow cytometry of apoptotic cell death. J. Immunol. Methods **243:**167–190.
74. **Wieser, J., B. N. Lee, J. W. Fondon, and T. H. Adams.** 1994. Genetic requirements for initiating asexual development in *Aspergillus nidulans*. Curr. Genet. **27:**62–69.
75. **Wyllie, A. H., J. F. R. Kerr, and A. R. Currie.** 1980. Cell death: the significance of apoptosis. Int. Rev. Cytol. **68:**251–306.
76. **Yu, J.-H., J. Wieser, and T. H. Adams.** 1996. The *Aspergillus* FlbA RGS domain protein antagonizes G protein signaling to block proliferation and allow development. EMBO J. **15:**5184–5190.
77. **Yun, D. J., J. I. Ibeas, H. Lee, M. A. Coca, M. L. Narasimhan, Y. Uesono, P. M. Hasegawa, J. M. Pardo, and R. A. Bressan.** 1998. Osmotin, a plant antifungal protein, subverts signal transduction to enhance fungal cell susceptibility. Mol. Cell **1:**807–817.
78. **Zhang, G., V. Gurtu, S. R. Kain, and G. Yan.** 1997. Early detection of apoptosis using a fluorescent conjugate of Annexin V. BioTechniques **23:** 525–531.
79. **Zurgil, N., Z. Schiffer, Y. Shafran, M. Kaufman, and M. Deutsch.** 2000. Fluorescein fluorescence hyperpolarization as an early kinetic measure of the apoptotic process. Biochem. Biophys. Res. Commun. **268:**155–163.
80. **Zurgil, N., Y. Shafran, D. Fixler, and M. Deutsch.** 2002. Analysis of early apoptotic events in individual cells by fluorescence intensity and polarization measurements. Biochem. Biophys. Res. Commun. **290:**1573–1582.
81. **Zurgil, N., I. Solodeev, B. Gilburd, Y. Shafran, E. Afrimzon, R. Avtalion, Y. Shoenfeld, and M. Deutsch.** 2004. Monitoring the apoptotic process induced by oxidized low-density lipoprotein in Jurkat T-lymphoblast and U937 monocytic human cell lines. Cell Biochem. Biophys. **40:**97–113.